FARADAY

Evanescent wave-induced fluorescence study of Rhodamine 101 at dielectric interfaces

A. J. de Mello,[a]* J. A. Elliott[b] and G. Rumbles[b]

[a] *School of Chemical Sciences, University of East Anglia, Norwich, UK NR4 7TJ*

[b] *Department of Chemistry, Imperial College of Science, Technology and Medicine, London, UK SW7 2AY*

Time-integrated and time-resolved evanescent wave-induced fluorescence spectroscopies (EWIFS) have been used to probe the photophysical properties of Rhodamine 101 at two solution/solid interfaces. Interaction of Rhodamine 101 with a fused silica surface leads to a reduction in the molecular fluorescence quantum efficiency in both cases. The fluorescence kinetics of interfacial species are shown to be complex (non-exponential), a function of bulk solution concentration, and a function of distance normal to the interface. The application of the maximum entropy method to the analysis of EWIF decays is presented. Recovered lifetime distributions expose inherent complexity and heterogeneity that is hidden to conventional analysis techniques.

Recently, much interest has been focussed around the study of molecular phenomena within interfacial environments.[1,2] An interface describes the boundary between two, homogeneous, immiscible phases. However, the 'interface' cannot be regarded as a simple geometrical plane, but rather as a three-dimensional region of characteristic thickness. In addition, although constructed from two bulk phases, the physical environment of an interface is quite distinct from that afforded by either medium alone. Consequently, the chemical and physical properties of molecular species within the interfacial environment are expected to be quite different from those in either of the constituent phases.

Various methodologies are available for probing surface and interfacial phenomena.[2] For example, techniques such as Auger electron spectroscopy (AES),[3] electron spectroscopy for chemical analysis (ESCA),[4] secondary ion mass spectrometry (SIMS),[4] low energy electron diffraction (LEED)[5] and scanning tunnelling microscopy (STM)[6] all exhibit extremely high sensitivity and selectivity when probing many solid surfaces.[7] Nevertheless, the suitability of a particular technique depends on the nature of the interface under investigation, and on the amount of information that the technique can provide. All the above methodologies, although highly sensitive, have significant drawbacks that prevent their universal adoption. In particular, most require high vacuum conditions (*i.e.* a non-ambient environment), destroy the sample under investigation or are not suited to the study of solid/liquid interfaces.

Surface analysis techniques utilising photons have gained considerable popularity in recent years. Importantly, these spectroscopic methods do not require highly specialised conditions, are generally non-destructive, and are well suited to the study of solid/liquid interfaces under ambient conditions. Of notable merit is evanescent wave-induced fluorescence spectroscopy (EWIFS).[8–10] EWIFS utilises total internal reflection of light to generate a surface-specific, electromagnetic disturbance (termed an evanescent wave) at the interface between the dielectric media. The evanescent wave is formed in the less dense medium, with its electric field amplitude decaying exponentially with distance normal to the interface. Subsequently, the evanescent wave is used to excite fluorophores selectively in the interfacial region (within *ca.* 500 nm of the geometric boundary).

Fluorescence spectroscopy is an exceptional technique used in the study of atomic and molecular phenomena. It is used routinely to probe molecular structure and conformation, molecular motion, energy transfer and solvent rearrangements, due primarily to its unrivalled sensitivity and high information content.[11] Consequently, it can be seen that the coupling of the evanescent wave with the method of fluorescence spectroscopy yields a highly sensitive method of probing interfacial environments.

Previously, EWIFS has been applied to the study of a variety of species in interfacial environments. These include polymers,[12,13] proteins,[14] dye molecules,[15,16] sub-micron particles,[17] and biological membranes.[18] The conventional approach is to relate time-integrated fluorescence information (emission intensities and spectral profiles) to the concentration and conformation of species in the evanescent volume. Even though EWIFS has proved useful in qualitatively analysing interfacial systems in this way, the very nature of the interface limits the measurement procedure. More precisely, an interface provides a heterogeneous environment for molecular species.[19] Hence, emission characteristics (such as molecular fluorescence quantum efficiencies) will be dependent on the precise location of individual fluorophores within this environment. Consequently, time-integrated measurements are limited, since even a 'simple' interface will almost certainly contain more than one type of fluorescent centre. To obtain a more complete understanding of the interface additional selectivity is required. This is achieved readily through time resolution. Now, variations in the photophysical properties of interfacial species can be detected through changes in the form of fluorescence decay profiles, and the spatial distribution of interfacial species can be mapped more closely.

Time-resolved evanescent wave-induced fluorescence spectroscopy (TREWIFS) has been used previously to probe interfacial photophysics. For example, TREWIF studies of molecular and polymeric species have demonstrated dramatic reductions or enhancements in fluorescence quantum efficiencies at dielectric interfaces.[15,16,20] Although these gross variations are measurable readily, the true nature of the modification is not fully understood. In particular, it is observed that in almost all situations, decay profiles describing interfacial fluorescence are far more complex than those resulting from species in the bulk phase. Lifetime distribution analysis (LDA) methods in conjunction with conventional sum-of-exponentials (SOE) analysis methods have been used recently to expose this complexity.[15,21,22] LDA methods allow differentiation of systems containing up to four discrete component populations and systems made up of a continuous distribution

of emitting species.[23] This paper addresses the issues of 'interfacial heterogeneity' and molecule–surface interactions by investigating the photophysical characteristics of the molecule Rhodamine 101 (R101) in bulk solution and at solid/solution interfaces. The fluorescence quantum efficiency of R101 in solution has been calculated to be virtually unity and independent of temperature.[24] Consequently, its use as a model fluorophore is widespread. Data are presented to illustrate the complexity of EWIF decay profiles, and surface perturbed fluorescence quantum efficiencies.

Experimental

R101 perchlorate (99.9%) was obtained from Lambda Physik and used without further purification. Aqueous solutions were made using doubly distilled water (Elgastat UHQ purified). All other solvents [Sigma and Aldrich (spectrophotometric or HPLC grade)] were tested for extraneous fluorescence and used without further purification. The molar decadic absorption coefficient of R101 in water was calculated to be 9.0×10^4 M^{-1} cm^{-1} at 572 nm.

Time-integrated EWIF measurements were performed on the EWIF spectrometer system shown in Fig. 1. Full details are given elsewhere.[22] Briefly, excitation is provided by a continuous wave (CW) argon ion laser (Spectra Physics 165). The sample is contained in a glass flow cell, and allowed to contact the surface of a hemicylindrical, fused silica prism (Spanoptic, $n_1 = 1.46$). The prism acts as the internal reflection element generating the evanescent wave in the less dense medium.

Before each experiment, the prism surface was made 'hydrophilic' (chemically and bacteriologically clean) using the following 'in-house' protocol: first, the surface was washed in copious amounts of acetone, ethanol, methanol and water, and then dried in a jet of N_2 gas. The prism was subsequently submerged in a chromosulfuric acid bath at 343 K for 60 min, washed in copious amounts of water, and dried in a jet of N_2 gas. At this stage, the prism surface was considered hydrophilic and was used within 12 h.

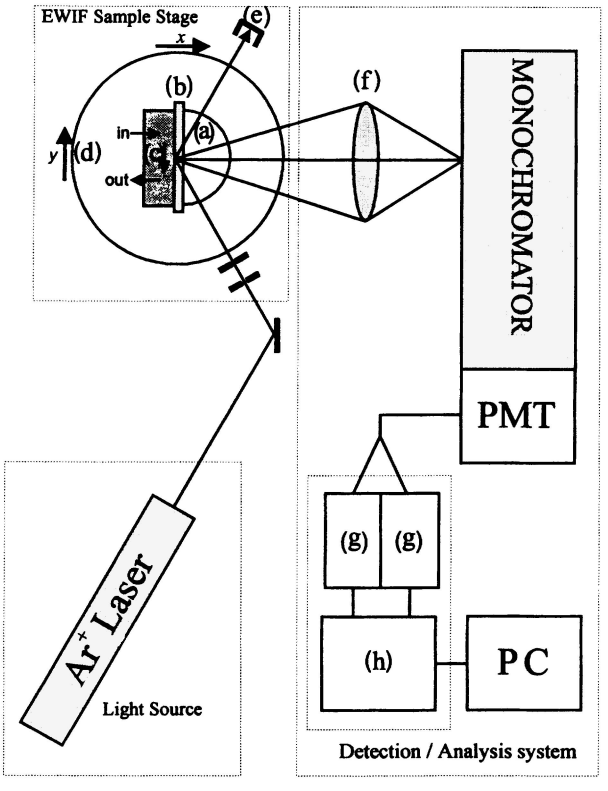

Fig. 1 Schematic of time-integrated EWIF spectrometer: (a) internal reflection element, (b) surface, (c) flow cell, (d) rotation stage, (e) beam stop, (f) collection optics, (g) constant fraction discriminator, (h) multichannel analyser

Time-integrated EWIF was detected and analysed using the technique of single-photon counting. Spectral selection was achieved using a 1 m double monochromator [Rank Hilger Monospek 1000 (0.8 Å mm^{-1}, reciprocal dispersion)], and the detection electronics consisted of a photomultiplier tube (Hamamatsu R928) and a two-channel, gated photon counter (Stanford Research Systems SR400).

Time-resolved EWIF measurements were recorded using the technique of time-correlated single-photon counting.[25] Full details of the system are described elsewhere.[22] Briefly, excitation light was provided by cavity dumped Rhodamine 6G and Rhodamine 110 dye lasers (Coherent 590/7200 CD and Coherent 700/7200 CD), pumped synchronously by the second harmonic of a mode-locked Nd : YAG laser (Coherent Antares 76-s). This produced a 3.8 MHz pulse train at 555–605 nm. The detection system consisted of a 0.22 m double monochromator (Spex 1681), microchannel plate (Photek 313 LJ), constant fraction discriminator (Ortec 584), time-to-amplitude converter (Ortec 547), and an MCA (Canberra Series 35 plus). Fluorescence decay profiles were collected to between 10 000 and 20 000 counts in the channel of maximum intensity (cmc). Decays were analysed using two methods.

Method 1: sum of exponentials. Decays were analysed as a sum of up to four exponential terms, using a normal iterative reconvolution routine based on the Levenberg–Marquardt algorithm.[26] Both pre-exponentials and decay times are variable parameters of the fitting routine. Plots of weighted residuals, autocorrelation function, serial correlation coefficient (DW) and reduced chi-square (χ^2) were used to judge the quality of the fit.

Method 2: lifetime distribution analysis. The maximum entropy method (MEM) was used to obtain the underlying lifetime distribution of the EWIF decay profiles.[27] The method assumes 100 exponents with fixed, logarithmically spaced lifetimes.

The fluorescence emission spectra in Fig. 2 were obtained using a single-photon counting spectrometer (Spex Fluoromax). The bandpass of both emission and excitation monochromators was 6 Å. The spectrum was corrected for variations in the lamp intensity as a function of time. Absorption spectra were recorded on a spectrophotometer [Perkin–Elmer (Lambda 2)], using a standard 10 mm pathlength cell.

Theory

When electromagnetic radiation propagating through a transparent, dielectric medium of refractive index n_1 encounters an interface with a similar medium of lower refractive index (n_2) at an angle greater than the critical angle [$\theta_c = \sin^{-1}(n_2/n_1)$], the radiation is totally internally reflected.[28] Nevertheless, solution of Maxwell's equations under these conditions predicts the existence of a non-propagating, transmitted field in medium 2.[29] The transmitted field is termed an evanescent wave, and has the general form

$$E(x) = E_0 \exp\left(\frac{-x}{d_p}\right) \quad (1)$$

where $E(x)$ is the electric field amplitude of the evanescent wave at a distance x from the interface, E_0 is the transmitted electric field amplitude per unit incoming amplitude, and d_p is the depth of penetration of the evanescent wave into medium 2. The depth of penetration is defined as the distance into medium 2 where the electric field amplitude of the evanescent wave has decreased to 1/e of its interfacial value, and is given by

$$d_p = \left(\frac{\lambda_{vac}}{2\pi n_1}\right)\sqrt{\left[\frac{1}{\sin^2\theta_1 - (n_2/n_1)^2}\right]} \quad (2)$$

As stated, the conceptual basis of EWIFS is the use of an evanescent wave to excite fluorophores within the interfacial environment (within *ca.* 500 nm of the geometrical interface). Therefore, medium 2 must be absorbing, *i.e.* energy is being extracted from the evanescent wave. Under these conditions, the refractive index of medium 2 becomes complex, and is given by

$$n_2 = n_2(1 + ik) \tag{3}$$

Here, n_2 (the real part) is the ordinary refractive index, and k is the attenuation index, which is related to the molar naperian absorption coefficient, α, by

$$k = \frac{\alpha\lambda}{4\pi n_2} \tag{4}$$

Consequently, an absorbing medium 2 modifies the transmitted field, and leads to a more complete expression for the depth of penetration, *i.e.*

$$d_{p,\,abs} = \frac{\lambda}{2\pi}\left[\frac{2}{-n_2^2(1-k^2) + n_1^2\sin^2\theta_i + \sqrt{[n_2^2(1-k^2) + n_1^2\sin^2\theta_i]^2 + 4n_2^4k^2}}\right]^{1/2} \tag{5}$$

Nevertheless, under most conditions it is sufficient to assume that the evanescent wave has the form given by eqn. (1). If the evanescent wave is used to excite fluorophores in the interfacial region, the evanescent wave-induced fluorescence intensity, I_f, can then be described by

$$I_f \propto \alpha \int_0^\infty \phi_f(x)c(x)I_0 \exp\left(-\frac{x}{\Lambda}\right) dx \tag{6}$$

where ϕ_f is the fluorescence quantum efficiency of the fluorophore, $c(x)$ is the fluorophore concentration profile in the x-direction, I_0 is the intensity of the evanescent wave at $x = 0$, and Λ the penetration depth of the evanescent wave ($d_p/2$). Therefore, if $\phi_f(x)$ is constant, evanescent wave-induced fluorescence intensity measurements relate directly to interfacial concentrations.

The fluorescence quantum efficiency is defined by

$$\phi_f = \frac{k_r}{k_r + k_{nr}} = k_r\tau_f \tag{7}$$

where k_r is the radiative deactivation rate coefficient, k_{nr} the non-radiative deactivation rate coefficient, and τ_f the fluorescence lifetime. Consequently, eqn. (6) can be rewritten as

$$I_f \propto k_r\alpha \int_0^\infty \tau_f(x)c(x)I_0 \exp\left(-\frac{x}{\Lambda}\right) dx \tag{8}$$

This refinement enables (i) changes in ϕ_f to be determined through measurement of τ_i and knowledge of k_r and (ii) interfacial concentrations to be directly related to EWIF intensity measurements.

Results

Solution photophysics of Rhodamine 101

The time-integrated absorption and emission spectra of R101 in water (1×10^{-5} M) are shown in Fig. 2. The principal absorption band is intense ($\varepsilon_{max} \approx 90\,000$ M^{-1} cm^{-1}), narrow and corresponds to the $S_0 \rightarrow S_1$ electronic, excitation transition ($\lambda_{max} = 572.4$ nm). The blue-edge shoulder at *ca.* 533 nm corresponds to a vibrational mode of the same $S_0 \rightarrow S_1$ excitation transition. The emission spectrum resembles closely the mirror image of the long wavelength absorption band ($\lambda_{max} =$ 598.6 nm). Furthermore, the Stokes' shift between the absorption and emission maxima is relatively small (765 cm^{-1}). Both these observations suggest a close similarity between the nuclear geometry of the ground-state and excited-state species, and support the idea of high molecular rigidity.

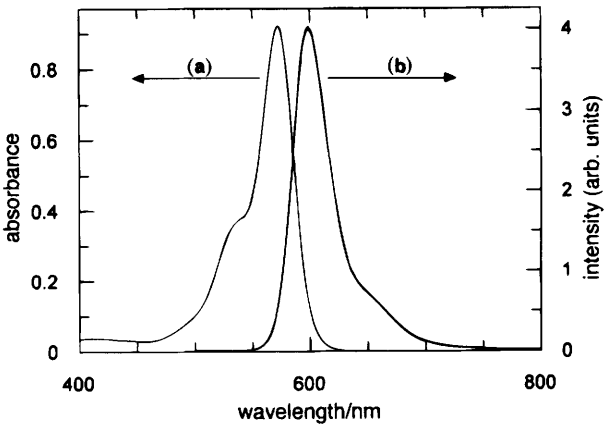

Fig. 2 Time-integrated spectra of R101 in water (concentration *ca.* 10^{-6} M). (a) Absorption spectrum, (b) emission spectrum, $\lambda_{ex} = 490$ nm.

Fig. 3 illustrates the bulk fluorescence decay profile of R101 in ethanol (1×10^{-7} M). Analyses, assuming a single exponential decay function, yield excellent fits at all levels of precision ($\tau_f = 4.05$ ns, $\chi^2 < 1.06$, DW > 1.84 and a c.m.c. of between 10^4 and 10^5). Bulk fluorescence decay measurements of R101 in water also yield excellent fits to a single exponential function. However, the resultant fluorescence decay time, $\tau_f = 3.90$ ns, is *ca.* 4% lower than that in ethanol. In addition, the magnitude of the fluorescence decay time is independent of both excitation and emission wavelengths. This fact demonstrates the existence of a single, emitting chromophore within the system.

Inspection of Fig. 2 illustrates a high degree of overlap between the absorption and emission spectra of R101 in solution. Furthermore, the molar absorption coefficient of R101 in solution is very large. Both these factors mean that emission measurements are prone to re-absorption (inner filter) effects. Such effects are well documented in the literature, although

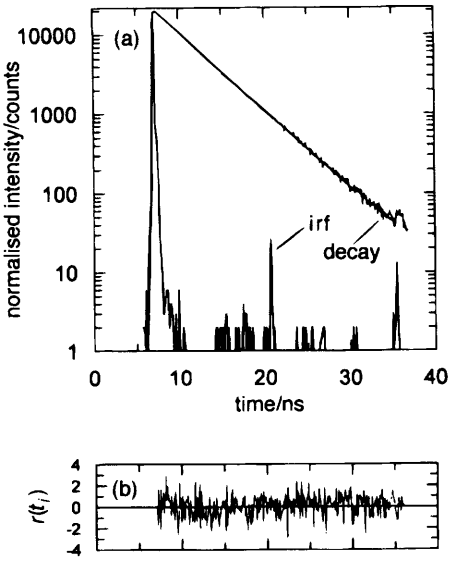

Fig. 3 Representative fluorescence decay profile of R101 in ethanol. Excitation wavelength = 555 nm, emission wavelength = 640 nm, c.m.c. = 2×10^4. (a) Decay curve, instrument response function (irf) and fitted function (straight line through the decay curve), (b) residuals for a single exponential fit to the data.

they are often overlooked in experiment.[30,31] The phenomenon of re-absorption acts to distort time-integrated emission spectra, and also to lengthen measured fluorescence decay times. These spectral and temporal distortions can be predicted using simple mathematical models.[30] Fig. 4 shows fluorescence decay profiles obtained for R101 in ethanol at four bulk solution concentrations (1.21×10^{-8} M–7.7×10^{-5} M). Solutions were contained in a standard 10×10 mm^2 cuvette, and fluorescence emission collected perpendicular to the direction of excitation. Without exception, all fluorescence decays are described by a single exponential decay function that is independent of emission wavelength. However, it can be seen clearly that the observed fluorescence decay time of R101 increases as the bulk solution concentration increases. This is owing solely to re-absorption of R101 monomer fluorescence, and not to any physical mechanism. If the increase in fluorescence decay time were due to the existence of additional emitting species (most likely dye aggregates), the fluorescence decay profile would be at least bi-exponential in nature (owing to the presence of more than one population of emitting species). In addition, the absorption spectra would also be likely to vary in shape if dye aggregates formed. These are not observed within the concentration range studied. Fig. 5 shows the normalised, bulk emission spectra (uncorrected) of R101 in ethanol at two concentrations. Here, the difference in spectral shape is due solely to the re-absorption of monomer emission.

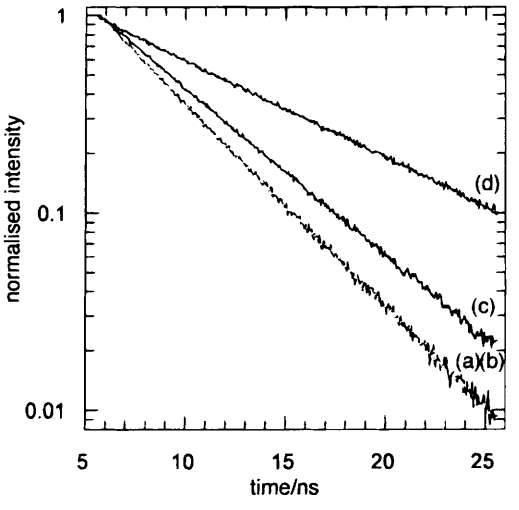

Fig. 4 Fluorescence decay profiles of R101 in ethanol at varying bulk solution concentrations: (a) 1.21×10^{-8} M, (b) 9.34×10^{-7} M, (c) 1.93×10^{-5} M, (d) 7.72×10^{-5} M

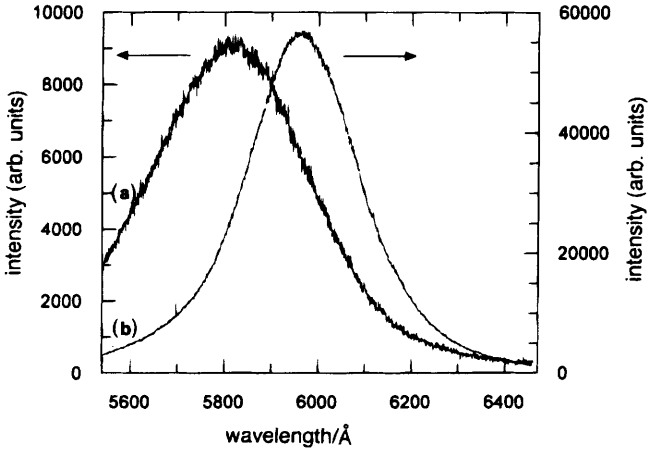

Fig. 5 Fluorescence emission spectra of R101 in ethanol. Excitation wavelength = 550 nm: (a) 6.1×10^{-7} M, (b) 2.4×10^{-5} M.

In other words, the gross effect of re-absorption is to cause a red shift in the emission maximum as the solution concentration increases.

Interfacial photophysics of Rhodamine 101

Time-integrated EWIF spectroscopy. EWIF spectra of R101 at an ethanol/fused silica interface were recorded for various bulk solution concentrations (6.0×10^{-7} M–1.5×10^{-5} M). Experimental conditions generate an evanescent wave with a penetration depth of *ca.* 77 nm. Fig. 6 shows three selected EWIF emission spectra. In all cases, the emission profiles are identical to the bulk solution emission spectrum at low concentration ($<10^{-7}$ M). The narrow features marked by asterisks are a result of Raman scattering from the surface of the fused silica prism (5553, 5917 and 6331 Å). The emission intensity increases as bulk solution concentration increases. However, it is noted that the rate of increase decreases with concentration. This observation suggests that either there is quenching of R101 fluorescence in the interfacial regime, or the 'interface' is filling up and allowing less molecules in per unit rise in bulk concentration.

At this point, it is interesting to note that the re-absorption phenomena seen in bulk solution are now absent (*i.e.* no red shift in the emission maximum). The reason for this lies in the nature of the evanescent wave. Re-absorption of fluorescence is dependent on the overlap between the absorption spectrum and the molecular fluorescence spectrum, the solution concentration, and the sample pathlength, l, through which molecular fluorescence photons have to travel before they escape the solution. For a given solution, the first two parameters will be

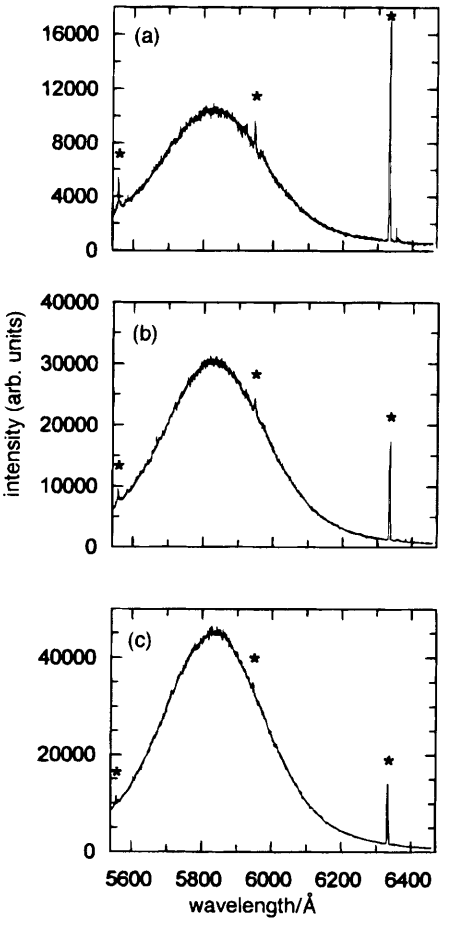

Fig. 6 EWIF spectra of R101 at a fused silica/ethanol interface. $d_p = 77$ nm. Solution concentrations: (a) 1.5×10^{-6} M, (b) 4.4×10^{-6} M, (c) 1.5×10^{-5} M.

Table 1 Parameters resulting from free SOE analyses of EWIF decay profiles of R101 at an ethanol/fused silica interface

conditions	concentration/M	τ_1/ps	τ_2/ps	A_1(%)	A_2(%)	$\langle\tau\rangle$/ns	χ^2	DW
bulk	9.5×10^{-7}	—	4043	—	100	4.04	1.15	1.84
EWIF	9.5×10^{-7}	1285	3857	16.2	83.8	3.70	1.07	2.24
EWIF	1.5×10^{-6}	1216	3783	20.8	79.2	3.58	1.11	2.03
EWIF	1.8×10^{-5}	1224	3767	27.4	72.6	3.49	1.07	1.70
EWIF	9.5×10^{-5}	1271	3784	31.1	68.9	3.45	1.17	1.65
EWIF	+1 wash	1081	3696	38.8	61.2	3.29	1.29	1.75

constant. Consequently, a decrease in l will reduce the extent of re-absorption. Thus, if l is made very small, high solution concentrations can be probed without experiencing re-absorption phenomena. For example, in a typical EWIFS experiment, l is of the order of 5×10^{-7} m. Hence, if $\varepsilon(\nu) \approx 90\,000$ M^{-1} cm^{-1}, a solution of concentration >0.1 M can be analysed without encountering any effects due to re-absorption! Accordingly, it is realised that EWIFS provides a simple way of measuring distortion-free emission spectra for high concentration solutions.

Time-resolved EWIF spectroscopy. To investigate the interfacial photophysics of R101 in more detail, time-resolved fluorescence measurements were performed. EWIF decays of R101 at an ethanol/fused silica interface were measured at four bulk solution concentrations. Subsequent to measurement at the highest solution concentration, solution is replaced by solvent, and an additional EWIF decay recorded. Table 1 summarises parameters resulting from successful SOE analyses. The fluorescence decay of R101 in bulk solution is measured as a calibration. Results demonstrate that although the fluorescence decay of R101 in bulk solution is well described by a single exponential decay function, all EWIF decay profiles require bi-exponential decay functions to generate fits of acceptable quality. In all cases, the first decay time component lies between 1081 and 1285 ps and the second decay time component lies between 3696 and 3857 ps. As bulk solution concentration increases the amplitude of the first component increases from 16% to *ca.* 31%, and the amplitude of the second component decreases from 84% to *ca.* 70%. This has the overall effect of lowering the average fluorescence decay time.

In many instances, the number of decay time components resulting from an SOE analysis is a reflection of the number of non-interacting fluorescent populations contributing to the decay. On this basis, there are two different R101 populations in the interfacial region: the major component representing a population whose characteristics are very similar to that of R101 in bulk solution (bulk species), and the second representing a population of quenched species, associated closely with the fused silica surface. To test this hypothesis, all data are re-analysed globally using a bi-exponential decay function, where the recovered decay times are common to all datasets. If the idea of two populations of emitting species is correct, then only the relative amplitudes of each component will change; the individual lifetimes will remain constant. In addition, it is noted that global analysis over a multidimensional data surface is as statistically rigorous a test of a particular model as can be performed.[22] Parameters resulting from this analysis are recorded in Table 2. Fits of excellent quality are obtained for all datasets. Thus on a statistical basis, there is strong evidence for the existence of two discrete molecular populations: one with a characteristic decay time of 1415 ps and one with a characteristic decay time of 3865 ps.

'Surface washing' causes a decrease in the average fluorescence decay time (Table 1). The introduction of solvent leads to the removal of bulk species as well as loosely adsorbed species. Subsequent to re-equilibration, the effective concentration of irreversibly adsorbed species (those with reduced fluorescence decay time) will therefore increase, and the average EWIF decay time will decrease.

In a similar study, EWIF decays of R101 at a water/fused silica interface were measured at four bulk solution concentrations. Subsequent to measurement at the highest solution concentration, solution is replaced by solvent, and an additional EWIF decay recorded. Table 3 summarises parameters resulting from successful SOE analyses. The results demonstrate that although the fluorescence decay of R101 in bulk solution is well described by a single exponential decay function, all EWIF decay profiles now require a tri-exponential decay law to generate fits of acceptable quality. In all cases, the first decay time component lies between 177 and 320 ps, the second decay time component lies between 954 and 1112 ps and the third decay time component lies between 3338 and 2708 ps. There is no systematic variation in the amplitudes. However, the overall effect is a decrease in the average EWIF decay time as the bulk solution concentration increases. Furthermore, 'surface washing' now causes an increase in the measured fluorescence decay time. This demonstrates that the affinity of R101 molecules for the fused silica surface is reduced when water is the solvent compared to when ethanol is used.

To investigate the validity of this description, the data were re-analysed globally, using a tri-exponential decay law. Parameters from this analysis are shown in Table 4. The analysis yields statistically adequate fits, with a global reduced χ^2 value of 1.17. It is observed that the relative amplitude of τ_3 decreases generally with bulk solution concentration. This causes an overall decrease in the average EWIF decay time as the solution concentration increases. Importantly, it is noted that none of the decay time components approximate the bulk solution decay time. This is somewhat surprising since the evanescent wave penetrates a significant distance into medium 2 (*ca.* four times the penetration depth, *i.e. ca.* 300 nm). With this in mind, a further global analysis is performed using a tetra-exponential decay function, where the final component is fixed to be the bulk solution decay time. Parameters resulting from this analysis are recorded in Table 5. The analysis yields statistically excellent fits, with a global reduced χ^2 value of 1.00. The relative amplitude of τ_4 decreases as 'surface concentration' increases. However, the relative amplitudes of τ_1, τ_2 and τ_3 do not show any systematic variations. This fact implies most likely that the recovered parameters are the result of pure curve parametrisation, and do not reflect the true physical characteristics of the emitting species.[23]

Table 2 Parameters resulting from a free bi-exponential, global analysis of EWIF decays of R101 at an ethanol/fused silica interface

	amplitude (%)				
conditions/M	$\tau_1 = 1415$ ps	$\tau_2 = 3805$ ps	$\langle\tau\rangle$/ns	χ^2	DW
9.5×10^{-7}	10.78	89.22	3.70	1.21	1.95
1.5×10^{-6}	19.34	80.66	3.61	1.10	2.01
1.8×10^{-5}	26.93	73.07	3.52	1.08	1.72
9.5×10^{-5}	32.20	67.80	3.45	1.09	1.65
+1 wash	39.70	60.30	3.34	1.28	1.86

Table 3 Parameters resulting from free SOE analyses of EWIF decay profiles of R101 at a water/fused silica interface

conditions	concentration/M	τ_1/ps	τ_2/ps	τ_3/ps	A_1(%)	A_2(%)	A_3(%)	$\langle\tau\rangle$/ns	χ^2	DW
bulk	1×10^{-7}	3901	—	—	100	—	—	3.90	1.03	2.06
EWIF	1×10^{-7}	177	1112	3321	53.7	28.2	18.1	2.34	1.10	1.83
EWIF	6.1×10^{-7}	250	1091	3089	43.6	34.1	22.3	2.19	1.01	2.02
EWIF	3.4×10^{-6}	242	954	2708	54.2	36.3	9.5	1.44	1.07	2.05
EWIF	0.7×10^{-5}	320	990	2768	63.6	29.9	6.5	1.26	1.19	1.78
EWIF	+1 wash	363	1654	3632	38.6	35.8	26.0	2.66	1.10	1.96

As stated in eqn. (2), variation of the angle of incidence yields a change in the penetration depth of the evanescent wave. Table 6 illustrates parameters resulting from a successful global analysis of selected EWIF decays of R101 at a water/fused silica interface, measured at varying angles of incidence. Statistically adequate fits are obtained for all datasets. The results show a dramatic decrease in the amplitude of τ_1 and increase in the amplitude of τ_3 as the angle of incidence decreases (*i.e.* penetration depth increases). This trend causes a lengthening of the average EWIF decay time as the angle of incidence decreases, and suggests that the interface can be visualised as consisting of three discrete populations of species with differing fluorescence decay times. The long decay time component (4001 ps) represents a molecular population whose characteristics are similar to those of R101 in bulk solution, whilst the other two decay time components describe R101 species interacting with the fused silica surface in some way. The short decay time component (617 ps) describes a population of highly quenched species that are irreversibly associated with the surface (on the timescale of the experiment), and the middle decay time component (2053 ps) represents species less strongly associated with the surface (further away from the geometrical interface). Fig. 7 illustrates the variation of the

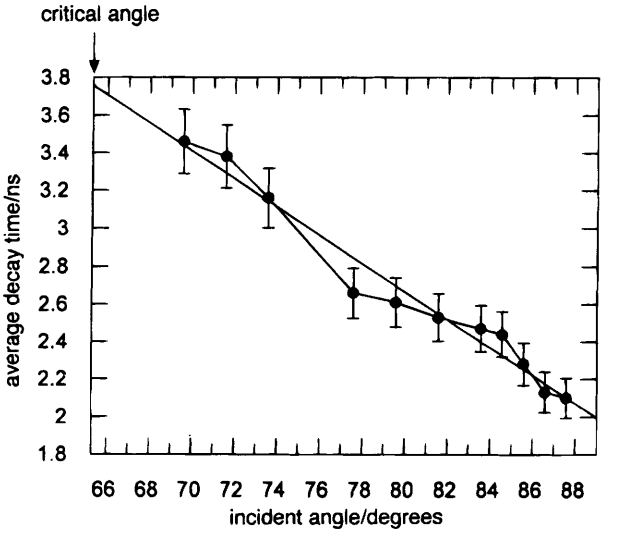

Fig. 7 Average EWIF decay time *vs.* angle of incidence for R101 at a water fused silica interface: solution concentration — 10^{-6} M

Table 4 Parameters resulting from a free tri-exponential, global analysis of EWIF decays of R101 at a water/fused silica interface

	amplitude (%)				
conditions/M	τ_1 = 352 ps	τ_2 = 1305 ps	τ_3 = 3387 ps	χ^2	DW
1×10^{-7}	58.56	25.79	15.65	1.07	1.78
6.1×10^{-7}	50.15	34.92	14.93	1.48	1.75
3.4×10^{-6}	61.27	33.28	5.45	0.94	1.81
0.7×10^{-5}	75.52	24.08	3.40	1.13	1.37
+1 wash	48.31	29.11	22.57	1.21	1.76

Table 5 Parameters resulting from a tetra-exponential, global analysis of EWIF decays of R101 at a water/fused silica interface (final component fixed to be 3880 ps)

	amplitude (%)					
decay	τ_1 = 259 ps	τ_2 = 906 ps	τ_3 = 2314 ps	τ_4 = 3880 ps	χ^2	DW
5	51.12	26.32	14.58	7.98	1.05	1.98
6	45.90	27.17	21.09	5.84	1.20	2.08
13	49.65	37.64	11.02	1.69	0.86	1.99
16	59.16	33.31	6.04	1.49	0.84	1.88
19	39.10	27.75	20.76	12.39	1.07	2.07

Table 6 Parameters resulting from a free tri-exponential, global analysis of EWIF decays of R101 at a water/fused silica interface: angle series

	amplitude (%)				
incident angle/degrees	τ_1 = 617 ps	τ_2 = 2053 ps	τ_3 = 4001 ps	χ^2	DW
87	82.84	13.47	3.69	1.34	1.86
85	72.29	21.14	6.56	1.10	1.90
81	58.59	29.98	11.43	1.34	2.17
79	51.63	32.23	16.14	1.03	1.98
73	40.91	26.10	32.99	1.04	1.97
69	32.44	21.39	46.17	1.18	1.92

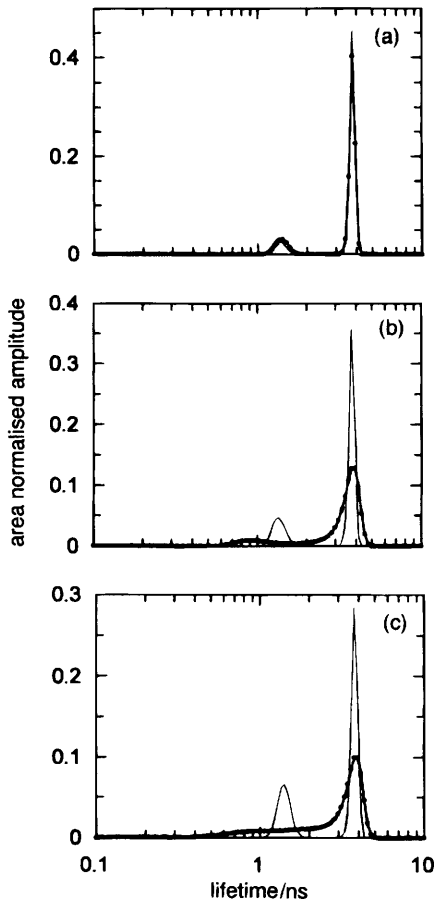

Fig. 8 MEM analyses of experimental and simulated EWIF decays of R101 at an ethanol/fused silica interface. Solution concentrations: (a) 1.6×10^{-6} M, (b) 1.8×10^{-5} M, (c) 9.5×10^{-5} M. Probe function of 100 terms over a 100–10000 ps range. (—●—) Experiment; (———) simulation.

average EWIF decay time $\langle\tau\rangle$ with incident angle. As stated, $\langle\tau\rangle$ increases as the incident angle decreases. Theoretically, the EWIF decay time at the critical angle should be representative of the bulk solution (since A is now infinite). Consequently, the data are fitted to a linear function, and extrapolated back to the critical angle (65.3°). According to this simple analysis, the predicted bulk fluorescence decay time is 3.78 ns. This is within 3% of the bulk solution value (3.90 ns). In addition, it is observed that the variation in $\langle\tau\rangle$ is gradual and continuous. This suggests that there may be a distribution of quenched species in the interfacial environment, rather than the three distinct populations as indicated by SOE analysis.

Extended analysis. Many studies have shown that the interpretation of fluorescence decay profiles is a non-trivial operation.[19,22,23] Analysis of decays using SOE methods may yield statistically adequate results, but provides no real information about the nature of the underlying lifetime distribution. An interface provides a particularly heterogeneous environment for a fluorophore. Conseqently, fluorescence decays resulting from an interfacial environment are likely to be more complex than an SOE description first implies. The decay laws recorded in Table 1–6 generally boast reduced χ^2 values of less than 1.3, and serial correlation coefficients above 1.7, *i.e.* all decay laws are of excellent quality. As long as a recovered decay law fulfils statistical requirements it is a valid description of the data. Accordingly, for a given decay, there will be a number of valid functions which comprise a feasible set.[27] This generates the problem of deciding which decay law gives the best description of the physical characteristics of an emitting system. Global analysis is helpful, since the recovered decay function must be able to describe adequately many sets of data. Nevertheless, multiple solutions still exist for a given dataset.

To address this problem in more detail, the MEM is applied to the analysis of EWIF decays of R101 near a fused silica surface. As illustrated previously, the MEM possesses the ability to uncover complexity in decay profiles which appear simple when examined using conventional SOE techniques.[15] The preferred solution is the one that introduces the fewest artifactual correlations into the chosen distribution.

For a model describing a set of n independent, emitting species, with lifetimes distributed in some arbitrary manner, a probe function can be represented by the sum

$$I(t) = \sum_{i=1}^{100} a_i \exp(-t/\tau_i) \tag{9}$$

i.e. 100 fixed, logarithmically spaced lifetimes (τ_i). Reconstruction of the amplitudes (a_i) is achieved by maximising the entropy-like function[32,33]

$$S = -\sum_{i=1}^{100} a_i \ln\left\{a_i \Big/ \sum_{i=1}^{100} a_i\right\} \tag{10}$$

The EWIF decays of R101 at an ethanol/fused silica interface described in Table 1 were analysed using the MEM. Distributions are constructed from 100 fixed, logarithmically spaced lifetimes between 100 and 10000 ps. In addition, bi-exponential, convoluted decays were simulated to describe the SOE decay laws recovered in Table 1 precisely. Precise details of synthetic decay curve generation are given elsewhere.[15,22,34] The synthetic, bi-exponential decays act as a control, and are analysed alongside the corresponding EWIF decays using the MEM. Selected, recovered lifetime distributions are illustrated in Fig. 8. In addition, Table 7 lists the

Table 7 Peak positions and peak area normalised amplitudes recovered from MEM analyses of EWIF decay profiles of R101 at an ethanol/fused silica interface

decay	concentration/M	peak/ns	area normalised amplitude (%)	peak/ns	area normalised amplitude (%)
experiment	9.5×10^{-7}	1.49	1.521	3.94	37.093
simulation	9.5×10^{-7}	1.42	6.565	3.76	58.797
experiment	1.5×10^{-6}	1.42	3.131	3.76	40.366
simulation	1.5×10^{-6}	1.42	5.509	3.76	45.291
experiment	1.8×10^{-5}	0.89	0.925	3.76	12.840
simulation	1.8×10^{-5}	1.35	4.767	3.76	35.657
experiment	9.5×10^{-5}	1.07	1.010	3.76	13.113
simulation	9.5×10^{-5}	1.35	2.997	3.76	32.370
experiment	+1 wash	—	—	3.94	9.947
simulation	+1 wash	1.29	1.672	3.76	28.483

peak positions and peak area normalised amplitudes for all recovered distributions.

At low bulk solution concentrations, the distributions recovered from experimental and simulated datasets are similar in shape [*e.g.* Fig. 8(a)]. Although discrimination of the two components is slightly better in the case of the simulated data, it is safe to assume that the bi-exponential description of the EWIF decay is valid. As the bulk solution concentration is increased, the recovered distributions remain bi-modal, but the short-time component distribution widens and shifts to shorter times [Fig. 8(b), (c)]. The long-time component, however, remains more defined in shape and stays fixed in time. These observations suggest a modified scenario to that encountered at low bulk solution concentrations.

In all cases, the long-time component almost certainly originates from species in bulk solution. As stated previously, the evanescent wave extends well into the solution phase. This means that almost all EWIF decays will contain some component representative of bulk phase species. Furthermore, since the bulk phase by definition is homogeneous, this component should be well defined and occur at *ca.* 4 ns in the distribution (the bulk solution decay time). This is observed. The short component recovered in the SOE analyses (Tables 1 and 2) was assumed to be representative of species interacting with the fused-silica surface. The MEM approach to decay-curve analysis shows this to be an incomplete description. The recovered lifetime distributions show that the short-time component broadens and shifts to shorter times as solution concentration increases. This broadening is indicative of a continuous distribution of emitting species, rather than a single population of quenched species. As the bulk solution concentration increases, more species enter the interfacial environment, and the observed heterogeneity in the fluorescence decay increases. Consequently, it can be seen that the application of SOE analysis methods to the analysis of EWIF decays provides little information about the underlying distribution of emitting species. The danger is that decays which are inherently complex can be parametrised by relatively simple SOE models.

Similar studies were performed for R101 at a water/fused silica interface. This time, tri-exponential, convoluted decays were simulated to describe precisely the SOE decay laws recovered in Table 3. Fig. 9 shows a selected lifetime distribution. It is observed that the distribution recovered from experimental data is completely different to that recovered from simulated data (in all cases). The distribution originating from the simulated dataset is trimodal, with maxima describing the individual-decay time components obtained from the original SOE analysis. This confirms that a true tri-exponential decay will yield a well defined, tri-modal lifetime distribution. The distribution resulting from experimental data is broad and continuous. This demonstrates significant heterogeneity within the interfacial regime. Nevertheless, there is still evidence of bulk species in the distribution (long-time component peak).

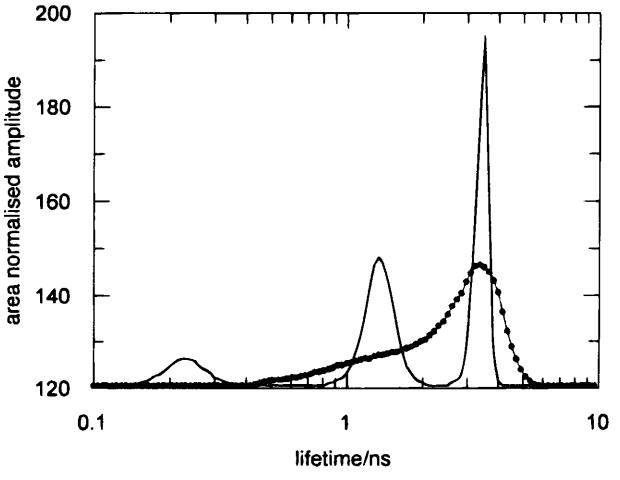

Fig. 9 MEM analysis of experimental and simulated EWIF decays of R101 at a water/fused silica interface. Solution concentration 1.6×10^{-6} M. Probe function of 100 terms over a 100–10000 ps range. (—●—) Experiment; (———) simulation.

Discussion

EWIFS has been applied successfully to the problem of discriminating between bulk-solvated and surface-associated species. In bulk solution, R101 boasts well defined photophysical characteristics. Its fluorescence quantum efficiency is unity, and independent of temperature. Furthermore, it exhibits a single exponential decay time of *ca.* 4 ns, which is independent of excitation and emission wavelength. There is no evidence for polymeric (aggregate) emission at high solution concentrations ($<10^{-4}$ M). Evanescent wave spectroscopic studies demonstrate that the interfacial photophysics of R101 are far more complex than the bulk solution photophysics. The results establish a number of interesting phenomena. First, interaction of R101 with a fused silica surface results in a reduction in the molecular fluorescence quantum efficiency. This is evidenced by a decrease in the average fluorescence decay time of R101 molecules (Tables 1–6). Second, all EWIF decays are non-exponential and require more complex decay functions to yield fits of acceptable quality. This demonstrates the heterogeneity of the interfacial environment. Variation of the depth of penetration of the evanescent wave indicates that species closely associated with the fused silica surface possess reduced fluorescence decay times, compared to species more associated with bulk solution (Fig. 7). This proves that the fluorescence quantum efficiency of R101 varies as a function of distance from the surface.

For both solvent systems studied, an increase in bulk solution concentration leads to a decrease in the amplitude of the longest decay time component, and an overall decrease in the average EWIF decay time. This behaviour is contrary to that of tetra-sulfonated aluminium phthalocyanine at a methanol/fused silica interface,[16] and shows that the influence of the surface on R101 molecules extends further into medium 2.

The final conclusions from this study relate to heterogeneity in the EWIF decay. First, all EWIF decays in this paper can be modelled successfully using bi- or tri-exponential decay laws (*i.e.* the fits are all of high statistical quality). Conventionally, the resulting decay times and pre-exponential factors are assigned to discrete emitting states or to parameters in a kinetic scheme. In other words, the recovered parameters are used to provide information about specific physical processes. The studies presented in this paper show that decays which are inherently complex can be parametrised by relatively simple SOE models. Consequently, little physical significance should be attributed to any parameters resulting from SOE analysis, unless supporting evidence is available (*e.g.* from the use of simulated decays).

The MEM analyses of EWIF decays at an ethanol/fused silica interface demonstrate that at low bulk solution concentrations EWIF decays are approximated adequately by bi-exponential decay laws. However, as the bulk solution concentration is increased, recovered lifetime distributions deviate from those retrieved from simulated datasets. They become broader and shift to shorter times, thus providing evidence for an underlying distribution of emitting species. At low bulk solution concentrations, the interface contains relatively few solute molecules which localise in specific sites. Hence, the EWIF decay is fairly simple. At higher bulk solution concentrations more solute molecules enter the interfacial environment, thus allowing a multitude of solute/surface and

solute/solute interactions to occur. Accordingly, the recovered distribution reflects this heterogeneity.

In summary, the heterogeneity in EWIF decay profiles uncovered by the MEM is not unexpected, and serves primarily to highlight the dangers of ascribing too much physical significance to parameters resulting from conventional SOE analyses. The most important challenge now faced is to interpret rather than expose the details of the inherent complexity of EWIF decays.

The authors would like to thank the Engineering and Physical Sciences Research Council (EPRSC) and Kodak UK Ltd for financial support for this work.

References

1 F. MacRitchie, in *Chemistry at Interfaces*, Academic Press, San Diego, 1990.
2 *Microchemistry: Spectroscopy and Chemistry in Small Domains*, ed. H. Masuhara, Elsevier Science BV, Amsterdam, 1994.
3 J. Czaux, *Vide-Sci. Tech. Applic.*, 1996, **64**, 65.
4 N. H. Turner and J. A. Screifels, *Anal. Chem.*, 1992, **64**, 302R.
5 K. Heinz, *Rep. Prog. Phys.*, 1995, **58**, 637.
6 (*a*) G. Binnig, *Rev. Mod. Phys.*, 1987, **59**, 615; (*b*) K. G. Tingey and J. D. Andrade, *Langmuir*, 1991, **7**, 2471.
7 K. G. Tingey and J. D. Andrade, *Langmuir*, 1991, **7**, 2471.
8 W. M. Reichert, *CRC Rev. Biocompatibility*, 1989, **5**, 173.
9 M. Toriumi and H. Masuhara, *Spectrochim. Acta Rev.*, 1991, **14**, 353.
10 A. J. de Mello, in *Surface Analytical Techniques for Probing Biomaterial Surface*, ed. J. Davies, CRC, Boca Raton, FL, 1996, in the press.
11 I. M. Warner, G. Patonay and M. P. Thomas, *Anal. Chem. A*, 1985, **57**, 463.
12 G. Rumbles, A. J. Brown, D. Phillips and D. Bloor, *J. Chem. Soc., Faraday Trans.*, 1992, **88**, 3313.
13 D. Aussere, H. Hervet and F. Rondelez, *Phys. Rev. Lett.*, 1985, **54**, 1948.
14 V. Hlady, *Appl. Spectrosc.*, 1991, **45**, 246.
15 A. J. de Mello, B. Crystall and G. Rumbles, *J. Colloid Interface Sci.*, 1995, **169**, 161.
16 G. Rumbles, A. J. Brown and D. Phillips, *J. Chem. Soc., Faraday Trans.*, 1991, **87**, 825.
17 E. H. Lee, R. E. Benner, J. B. Benn and R. K. Chang, *Appl. Opt.*, 1979, **18**, 862.
18 C. L. Poglitsch and N. L. Thompson, *Biochemistry*, 1990, **29**, 248.
19 D. R. James, Y. S. Liu, P. De Mayo and W. R. Ware, *Chem. Phys. Lett.*, 1985, **120**, 460.
20 M. A. Bell, B. Crystall, G. Rumbles, G. Porter and D. R. Klug, *Chem. Phys. Lett.*, 1994, **221**, 15.
21 Y. S. Liu and W. R. Ware, *J. Phys. Chem.*, 1993, **97**, 5980.
22 A. J. de Mello, PhD Thesis, University of London, 1995.
23 D. R. James and W. R. Ware, *Chem. Phys. Lett.*, 1986, **126**, 7.
24 J. Karpiuk, Z. R. Grabowski and F. C. de Schryver, *J. Phys. Chem.*, 1994, **98**, 3247.
25 D. V. O'Connor and D. Phillips, in *Time-Correlated Single Photon Counting*, Academic Press, London, 1984.
26 D. W. Marquardt, *J. Soc. Ind. Appl. Math.*, 1963, **11**, 431.
27 A. K. Livesey and J. C. Brochon, *Biophys. J.*, 1987, **52**, 693.
28 M. Born and E. Wolf, in *Principles of Optics*, Pergamon Press, Oxford, 1970.
29 J. C. Maxwell, in *A Treatise on Electricity and Magnetism*, Dover, Oxford, 1873, vol. 1–2.
30 J. B. Birks, in *Photophysics of Aromatic Molecules*, Wiley, New York, 1970.
31 S. Dhami, A. J. de Mello, G. Rumbles, S. M. Bishop, D. Phillips and A. Beeby, *Photochem. Photobiol.*, 1995, **61**, 341.
32 *Maximum Entropy and Bayesian Methods in Inverse Problems*, ed. C. R. Smith and W. T. Grady Jr., Reidel, Boston, 1985.
33 A. Siemiarczuk, B. D. Wagner and W. R. Ware, *J. Phys. Chem.*, 1990, **94**, 1661.
34 T. A. Smith and M. Carey, personal communication.

Paper 6/04838B; *Received* 9*th July*, 1996